

# Measured optical constants of copper from 10 nm to 35 nm

Nicole Brimhall, Nicholas Herrick, David D. Allred, R. Steven Turley,  
Michael Ware, and Justin Peatross\*

*Department of Physics and Astronomy, Provo, UT 84602, U.S.A.*

[\\*peat@byu.edu](mailto:*peat@byu.edu)

**Abstract:** We use laser high-order harmonics and a polarization-ratio-reflectance technique to determine the optical constants of copper and oxidized copper in the wavelength range 10-35 nm. This measurement resolves previously conflicting data sets, where disagreement on optical constants of copper in the extreme ultraviolet most likely arises from inadvertent oxidation of samples before measurement.

© 2009 Optical Society of America

**OCIS codes:** (340.7480) X-rays, soft x-rays, extreme ultraviolet (EUV); (240.2130) Ellipsometry and polarimetry; (160.4760) Optical properties; (160.3900) Metals; (190.2620) Harmonic generation and mixing .

---

## References and links

1. K. Maex, M. R. Baklanov, D. Shamiryan, F. Iacopi, S. H. Brongersma, and Z. S. Yanovitskaya, "Low dielectric constant materials for microelectronics," *J. Appl. Phys.* **93**, 8793-8841 (2003).
2. V. M. Dubin, R. Akolkar, C. C. Cheng, R. Chebiam, A. Fajardo, F. Gstrein, "Electrochemical materials and processes in Si integrated circuit technology," *Electrochim. Acta* **52**, 2891-2897 (2007).
3. D. Gimenez-Romero, J. J. Garcia-Jareno, J. Agrisuelas, C. Gabrielli, H. Perrot, and F. Vicente, "Formation of a Copper Oxide Layer as a Key Step in the Metallic Copper Deposition Mechanism," *J. Phys. Chem. C* **112**, 4275-4280 (2008).
4. J. Shin, H. W. Kim, K. Agapiou, R. A. Jones, G. S. Hwang, and J. G. Ekerdt, "Effects of P on amorphous chemical vapor deposition Ru-P alloy films for Cu interconnect liner applications," *J. Vac. Sci. Technol. A* **26**, 974-979 (2008).
5. W. A. Lanford, P. J. Ding, W. Wang, S. Hymes, and S. P. Murarka, "Alloying of copper for use in microelectronic metallization," *Mater. Chem. Phys.* **41**, 192-198 (1995).
6. M. Surya Sekhar and S. Ramanathan, "Characterization of copper chemical mechanical polishing (CMP) in nitric acidhydrazine based slurry for microelectronic fabrication," *Thin Solid Films* **504**, 227-230 (2006).
7. C. Gabrielli, C. Mace, E. Ostermann, and A. Pailleret, "AFM Characterization of Copper Dendritic Growths in Integrated Electronic Microcircuits," *Electrochem. Solid-State Lett.* **11**, D5-D8 (2008).
8. R. Gras, L. G. Gosset, E. Petitprez, V. Girault, M. Hopstaken, S. Jullian, G. Imbert, Y. Le Fric, J. Bienacel, J. Guillan, T. Chevolleau, S. Sherman, M. Tabat, J. Hautala and J. Torres, "Integration and characterization of gas cluster processing for copper interconnects electromigration improvement," *Microelectron. Eng.* **84**, 2675-2680 (2007).
9. R. Soufli, R. M. Hudyma, E. Spiller, E. M. Gullikson, M. A. Schmidt, J. C. Robinson, S. L. Baker, C. C. Walton, and J. S. Taylor, "Sub-diffraction-limited multilayer coatings for the 0.3 numerical aperture micro-exposure tool for extreme ultraviolet lithography," *Appl. Opt.* **46**, 3736-3746 (2007).
10. B. Wu and A. Kumar, "Extreme ultraviolet lithography: A review," *J. Vac. Sci. Technol. B* **25**, 1743-1761 (2007).
11. D. Attwood, "Extreme Ultraviolet Light Sources for Semiconductor Manufacturing," *J. Phys. D* **37**, 3233 (2004).
12. International Technology Roadmap for Semiconductors, <http://www.itrs.net/Links/2007ITRS/Home2007.htm> (2007 Edition, accessed 18 August 2009).
13. H. J. Hagemann, W. Gudat, and C. Kunz, "Optical constants from the far infrared to the x-ray region: Mg, Al, Cu, Ag, Au, Bi, C, and Al<sub>2</sub>O<sub>3</sub>," *J. Opt. Soc. Am.* **65**, 742 (1975).
14. R. Haensel, C. Kunz, T. Sasaki, and B. Sonntag, "Absorption Measurements of Copper, Silver, Tin, Gold, and Bismuth in the Far Ultraviolet," *Appl. Opt.* **7**, 301-306 (1968).
15. D. H. Tomboulou, D. E. Bedo, and W. M. Neupert, "M<sub>2,3</sub> absorption spectra of the elemental solids Cr through Ge," *J. Phys. Chem. Solids* **3**, 282 (1957).

16. D. Beaglehole, M. De Crescenzi, M. L. Theye, and G. Vuye, "Dielectric constant of gold, copper, and gold-copper alloys between 18 and 35 eV," *Phys. Rev. B* **19**, 6303 (1979).
  17. <http://henke.lbl.gov/opticalconstants/> (accessed 16 June 2009).
  18. N. Brimhall, M. Turner, N. Herrick, D. D. Allred, R. S. Turley, M. Ware, and J. Peatross, "Extreme-ultraviolet polarimeter utilizing laser-generated high-order harmonics," *Rev. Sci. Instr.* **79**, 103108-1-7 (2008).
  19. N. Brimhall, N. Heilmann, M. Ware, and J. Peatross, "Polarization-ratio reflectance measurements in the extreme ultraviolet," *Opt. Lett.* **34**, 1429-1431 (2009).
- 

## 1. Introduction

Copper recently replaced aluminum as the material of choice for on-chip interconnections [1–4] because of its low resistivity, ease of deposition, high thermal conductivity, and high electromigration resistance [1, 2, 5]. This transition has increased the need to accurately characterize the material properties of copper [6–8]. In particular, with the push to move to extreme ultraviolet (EUV) wavelengths for lithography [9–11], it is desirable to have an accurate characterization of the optical properties of copper in the EUV for the sake of lithographic image modeling. According to the International Technology Roadmap for Semiconductors [12], lithography is expected to move from its current wavelength of 193 nm to an EUV wavelength of 13.5 nm in order to manufacture smaller features. While the EUV optical constants of copper have previously been measured at this wavelength [13–15] and at other EUV wavelengths [16], there are significant discrepancies between the data sets of EUV optical constants.

In this article we resolve these discrepancies and present the optical constants of copper and copper (II) oxide in the range from 10 nm to 35 nm. We find that the most widely cited optical constants for copper in the EUV, those reported by Hagemann *et al.* [13] and referenced on the Center for X-ray Optics (CXRO) website [17], are actually the optical constants of oxidized copper, in spite of an attempt to prevent oxidation with a capping layer. Similarly, Haensel *et al.* [14] obtained the optical constants of oxidized copper in this range while representing them to be those of copper (although they do not report taking any measures to prevent sample oxidation). On the other hand, our measurements for copper agree with those made by Tomboulian [15] and Beaglehole [16]. However, their wavelength ranges covered only a small portion of the EUV. Thus, we report what we believe to be the first accurate characterization of the constants for copper through most of EUV wavelength range. We also report the first (intentional) characterization of oxidized copper in this range. This is the first time that the EUV optical constants of both copper and oxidized copper have been compared in the same instrument.

## 2. Measurement Method

We made these measurements using the laser-high-harmonics-based polarimeter described in Ref. [18] and the polarization-ratio-reflectance method described in Ref. [19]. This instrument uses high-intensity laser pulses (800 nm, 10 mJ, 35 fs at 10 Hz) focused into a noble gas to produce polarized and directional high-harmonics with wavelengths distributed throughout the EUV. The polarimeter is a compact and low-cost alternative to synchrotron-based systems for making reflectance measurements, and allows for *in situ* measurements during the thin-film deposition process. We recently modified our instrument to include evaporation equipment so that thin-film samples can remain under vacuum between deposition and measurement. Since reflectance measurements can be made a few minutes after deposition and without breaking vacuum, this instrument provides a reliable method for characterizing unoxidized metal films.

We measured the optical constants of copper films deposited on polished silicon (100) substrates. The silicon substrates were naturally oxidized, with SiO<sub>2</sub> layers between 1 nm and 3 nm (measured with spectroscopic ellipsometry). To avoid hydrocarbon contamination, the substrates were cleaned with a xenon excimer lamp for five minutes immediately before pump-

ing down the system. After pumping down and initial optical alignment, the sample substrate was rotated until it pressed against an o-ring on a bellows leading to the deposition chamber. This created a seal that temporarily isolated the deposition region from the reflectance chamber. The deposition chamber was then evacuated further with a sorption pump to a pressure of  $< 10^{-5}$  torr. Approximately 5 g of copper (99.99% purity) was evaporated horizontally using a tungsten basket onto the substrates at a distance of 35 cm, producing a film thickness between 7 nm and 12 nm. With thinner films, we found that the copper would agglomerate on the surface, forming tiny islands instead of providing uniform coverage. This is presumably a surface effect, which we avoided by using thicker samples.

After deposition, we rotated the sample away from the deposition chamber and made reflectance measurements as the grazing angle was varied (at room temperature and  $10^{-4}$  torr). At each angle we measured the reflected signal of both p- and s-polarized light for each wavelength in the spectral comb, and computed the ratio of the p- and s-polarized reflectances. Because there was little time delay between measurements for the two polarizations, this ratio divides away variations in incident intensity and other systematic measurement errors that may affect both measurements [19]. (Rotatable polarization is a unique advantage of our EUV source.) We made reflectance-ratio measurements at wavelengths from 10 nm to 35 nm with grazing angles from 0 to 45 degrees. At each angle, 400 laser shots were averaged at an effective frequency of about 3 Hz (owing to energy discrimination of our 10 Hz laser source as described in Ref. [18]).

After reflectance-ratio measurements were made, the copper samples were exposed to atmosphere and quickly characterized using a near-visible spectroscopic ellipsometer (Wollam Woollam M2000) to determine the thickness of the metal and the oxide layer that had formed since air exposure. The first measurement was made five minutes after exposure, and the oxide layer at this time was found to be about 0.7 nm thick. We continued making measurements at two minute intervals, and observed the oxide layer growing at a rate of about 0.02 nm/minute. Samples were then heated to about 150°C for 5 minutes, after which spectroscopic ellipsometry indicated that they were fully oxidized. The fully oxidized samples were returned to the polarimeter and a series of reflectance ratios were measured for the oxidized copper.

We measured the roughness of the oxidized films using atomic force microscopy (AFM), which showed that the films had a roughness less than 1 nm (RMS) on a  $1 \mu\text{m} \times 1 \mu\text{m}$  scale. Using spectroscopic ellipsometry, we found that the uniformity across 1 cm of the deposited film was about  $\pm 0.2$  nm. The high-harmonics spot size at the sample was about 1 mm in diameter. Thus, at a 5 degree sample angle, the extent of the beam across the sample was about 1 cm.

To determine the composition of the oxide layer, we measured the near-visible-wavelength optical constants using spectroscopic ellipsometry. These measured constants matched well with the accepted values for CuO but poorly with other copper oxides. We also examined similarly-prepared samples using x-ray photoemission spectroscopy (XPS). We found that the XPS spectrum of the fully oxidized copper layer matched that of CuO well but was a poor match to other copper oxides. Finally, the oxide layer appeared visually black, which is consistent with being composed of CuO rather than CuO<sub>2</sub> (which appears red). We thus conclude that the oxide layer was essentially composed of CuO. Of course, there will always be some level of other compounds present in the oxide layer, but our sample should be typical of a naturally oxidized copper film.

### 3. Results

The optical constants for Cu and CuO were calculated by using nonlinear regression (implemented by the `nlinfit` command in Matlab) to fit the reflectance-ratio data to the multilayer

reflectance model outlined in Ref. [19]. Figure 1 shows the optical constants with error bars representing the 95% confidence intervals for  $n$  or  $\kappa$  from the nonlinear regression analysis. Numerical values for these measurements are given in Table 1.

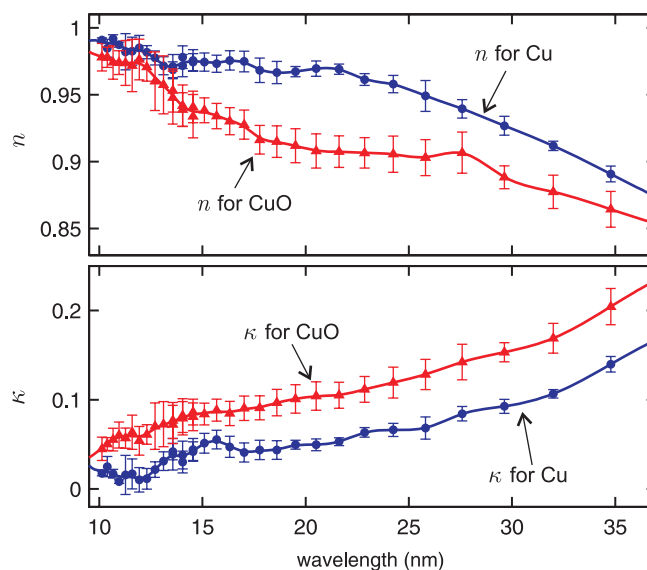


Fig. 1. The optical constants of Cu and CuO determined using the ratio reflectance technique. Statistical error bars are also shown.

In this analysis, the interface between the copper (or copper oxide) layer and the substrate was taken to be ideal (sharp). The optical constants  $n$  and  $\kappa$  for the Cu (or CuO) layer were taken as fit parameters while the optical constants for the silicon dioxide layer and silicon substrate were treated as fixed parameters. The thickness of the fully oxidized film (which was characterized using spectroscopic ellipsometry as described above) was held fixed during the fit. The uncertainty in this thickness (including uncertainty in the ellipsometric fit and non-uniformity across the sample) was  $\pm 0.3$  nm. The thickness of the unoxidized copper film was taken to include the thickness of the oxide layer that formed between exposure to air and thickness measurement, but decreased according to the ratio of bulk densities,  $6.31 \text{ g/cm}^3$  for CuO to  $8.96 \text{ g/cm}^3$  for Cu. We estimate that the Cu layer thickness was accurate to  $\pm 0.7$  nm, owing to uncertainties in the density and/or composition of the oxide, variation across the sample, and uncertainties in the ellipsometry fit.

To determine how much uncertainties in film thickness could affect values for optical constants, we re-fit each data set for the maximum and minimum thicknesses set by our uncertainties (with the thickness fixed) to see how much our fit values for optical constants changed. At an example wavelength,  $\lambda = 15.1$  nm ( $q = 53$ ), changing the thickness by  $\pm 0.7$  nm changed  $n$  by  $\pm 0.0026$  and  $\kappa$  by  $\pm 0.0052$  (about a 10% variation in either  $\kappa$  or  $1 - n$ ). At each wavelength we added in quadrature the statistical error due to the fit and this error due to uncertainty in the film thickness. Total error for values of  $n$  was typically about 0.009, and total error for values of  $\kappa$  was typically about 0.01.

When measuring thinner samples of some other materials after exposure to room air, we sometimes have found it necessary to include the possibility of a thin carbon contamination layer when fitting the data [19]. This possibility had negligible impact on the fits to our CuO measurements (and is not applicable to our Cu measurements).

Table 1. Measured optical constants for Cu and CuO.

wavelength	$n$ for Cu	$\kappa$ for Cu	$n$ for CuO	$\kappa$ for CuO
42.1	$0.874 \pm 0.013$	$0.236 \pm 0.012$		
38.1	$0.880 \pm 0.013$	$0.184 \pm 0.010$		
34.8	$0.891 \pm 0.010$	$0.140 \pm 0.010$	$0.864 \pm 0.016$	$0.204 \pm 0.021$
32.0	$0.912 \pm 0.009$	$0.107 \pm 0.006$	$0.877 \pm 0.015$	$0.169 \pm 0.017$
29.6	$0.927 \pm 0.010$	$0.093 \pm 0.009$	$0.888 \pm 0.011$	$0.153 \pm 0.011$
27.6	$0.940 \pm 0.009$	$0.084 \pm 0.008$	$0.907 \pm 0.016$	$0.142 \pm 0.020$
25.8	$0.949 \pm 0.012$	$0.068 \pm 0.013$	$0.903 \pm 0.014$	$0.128 \pm 0.017$
24.2	$0.958 \pm 0.007$	$0.066 \pm 0.008$	$0.906 \pm 0.014$	$0.119 \pm 0.017$
22.9	$0.961 \pm 0.005$	$0.063 \pm 0.006$	$0.907 \pm 0.012$	$0.112 \pm 0.015$
21.6	$0.969 \pm 0.004$	$0.053 \pm 0.005$	$0.908 \pm 0.012$	$0.105 \pm 0.015$
20.5	$0.970 \pm 0.006$	$0.050 \pm 0.007$	$0.908 \pm 0.013$	$0.104 \pm 0.016$
19.5	$0.967 \pm 0.005$	$0.050 \pm 0.007$	$0.912 \pm 0.013$	$0.101 \pm 0.017$
18.6	$0.967 \pm 0.009$	$0.044 \pm 0.012$	$0.915 \pm 0.012$	$0.097 \pm 0.016$
17.8	$0.968 \pm 0.010$	$0.044 \pm 0.012$	$0.916 \pm 0.011$	$0.091 \pm 0.014$
17.0	$0.975 \pm 0.008$	$0.041 \pm 0.011$	$0.928 \pm 0.011$	$0.091 \pm 0.014$
16.3	$0.976 \pm 0.007$	$0.047 \pm 0.012$	$0.930 \pm 0.010$	$0.085 \pm 0.014$
15.7	$0.973 \pm 0.007$	$0.055 \pm 0.011$	$0.934 \pm 0.010$	$0.088 \pm 0.013$
15.1	$0.974 \pm 0.007$	$0.051 \pm 0.012$	$0.938 \pm 0.010$	$0.084 \pm 0.013$
14.5	$0.976 \pm 0.009$	$0.044 \pm 0.013$	$0.934 \pm 0.016$	$0.086 \pm 0.015$
14.5	$0.974 \pm 0.007$	$0.042 \pm 0.012$	$0.941 \pm 0.012$	$0.081 \pm 0.017$
14.0	$0.978 \pm 0.009$	$0.038 \pm 0.017$	$0.939 \pm 0.013$	$0.082 \pm 0.020$
14.0	$0.972 \pm 0.009$	$0.030 \pm 0.014$	$0.942 \pm 0.016$	$0.079 \pm 0.020$
13.6	$0.971 \pm 0.010$	$0.039 \pm 0.020$	$0.948 \pm 0.020$	$0.072 \pm 0.023$
13.6	$0.969 \pm 0.008$	$0.042 \pm 0.013$	$0.953 \pm 0.017$	$0.077 \pm 0.022$
13.1	$0.972 \pm 0.009$	$0.031 \pm 0.014$	$0.957 \pm 0.022$	$0.073 \pm 0.027$
12.7	$0.978 \pm 0.007$	$0.022 \pm 0.012$	$0.960 \pm 0.022$	$0.070 \pm 0.028$
12.3	$0.982 \pm 0.008$	$0.011 \pm 0.015$	$0.971 \pm 0.012$	$0.061 \pm 0.014$
11.9	$0.985 \pm 0.011$	$0.010 \pm 0.016$	$0.976 \pm 0.016$	$0.054 \pm 0.018$
11.6	$0.983 \pm 0.012$	$0.017 \pm 0.019$	$0.972 \pm 0.020$	$0.064 \pm 0.021$
11.3	$0.982 \pm 0.015$	$0.016 \pm 0.024$	$0.974 \pm 0.018$	$0.057 \pm 0.015$
11.0	$0.987 \pm 0.006$	$0.008 \pm 0.011$	$0.974 \pm 0.011$	$0.060 \pm 0.018$
10.7	$0.992 \pm 0.008$	$0.017 \pm 0.011$	$0.974 \pm 0.014$	$0.055 \pm 0.016$
10.4	$0.985 \pm 0.010$	$0.025 \pm 0.016$	$0.978 \pm 0.010$	$0.050 \pm 0.013$
10.1	$0.991 \pm 0.008$	$0.017 \pm 0.011$	$0.978 \pm 0.013$	$0.045 \pm 0.017$

#### 4. Comparison to Previous Reports

We are aware of four other reports on the optical constants of copper in this wavelength range. Hagemann *et al.* [13] performed transmittance measurements using the DESY synchrotron as a light source between 13 eV and 150 eV photon energies. The samples were prepared by vacuum evaporation as thin films; the thickness ranged from less than 100 Å to 600 Å. In an attempt to prevent subsequent oxidation of the samples, they evaporated 50 Å carbon *in situ* onto both sides of the films.

Haensel *et al.* [14] prepared samples by evaporating spectroscopically pure metals from tungsten and tantalum boats onto Zapon foils (about 500 Å thick) supported by a fine copper mesh. The film thickness was monitored by a quartz oscillator during evaporation and ranged in thick-

ness from 50 Å to 6500 Å. For about thirty discrete wavelengths within the range 50 Å to 340 Å the ratio of the foil transmittance divided by the Zapon reference foil transmittance was evaluated. The light source was also the DESY synchrotron.

Beaglehole *et al.* [16] determined optical constants by measuring reflection from electropolished bulk samples at four angles of incidence for light for photon energies between 18 eV and 35 eV. The light source was a spark discharge in argon. Samples were heated in vacuum to 400 C to remove the surface oxide layer.

Finally, Tomboulian *et al.* [15] evaporated copper samples on Zapon foils (thicknesses were several hundred angstroms). Absorption measurements were performed in the wavelength range 10 to 20 nm with a spark discharge plasma as the source.

Figure 2 shows a plot of our measured  $n$  and  $\kappa$  for Cu and CuO compared with the values given in these four reports. Hagemann, Haensel, and Tomboulian measured photoabsorption only, so they only obtained values for  $\kappa$ . Our measured  $n$  and  $\kappa$  for copper show agreement with data measured *in situ* by Beaglehole (where the data overlap on the long-wavelength end). It is noteworthy that Beaglehole is the only of the four references that made *in situ* measurements, as did we. This type of measurement is very reliable at preventing oxidation since the sample remains under vacuum through the entire deposition and measurement process.

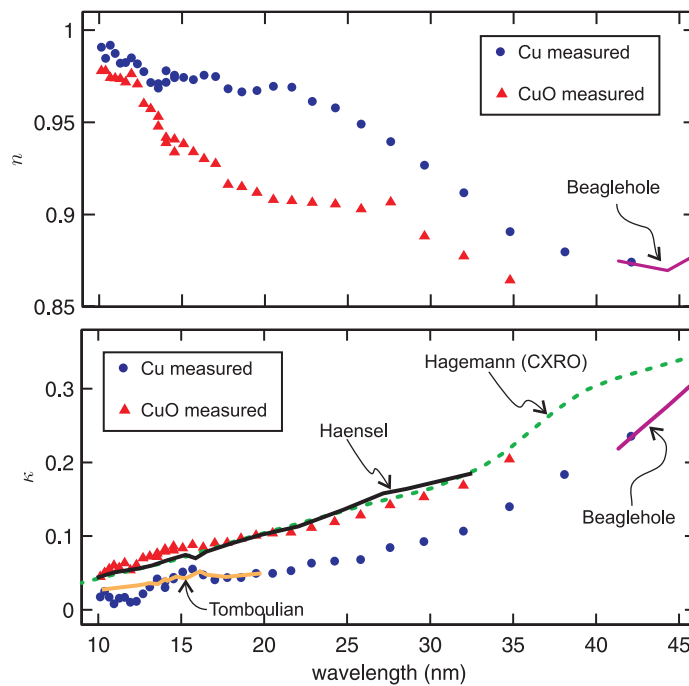


Fig. 2. Our measured  $n$  and  $\kappa$  for Cu and CuO compared with other reported values for copper. Our values for Cu match those of Beaglehole (measured *in situ*) and Tomboulian (not measured *in situ*) within our error bars. Our values for oxidized copper match those of Haensel (not measured *in situ*) and Hagemann (measured with a carbon capping layer).

Our data for unoxidized copper metal also matches the values measured by Tomboulian (with data overlap on the short wavelength end). This was somewhat unexpected, since his samples were exposed to air before measurement. However, Tomboulian described that the samples were exposed to air for only a short period of time, whereas his samples were  $>50$  nm thick. Based on our observations, if the samples were only exposed to air for a few minutes, they

may have only oxidized  $<1$  nm in depth, leaving a very high percentage of the sample as pure copper.

In contrast, the values reported by Hagemann for Cu match our measurements of CuO rather than Cu. Hagemann's samples were relatively thin; some thicknesses were less than 10 nm. Hagemann and coworkers aimed to prevent sample oxidation by coating their copper samples with 5 nm carbon capping layers on both sides of the film. However, by comparing with our measured data it seems that their samples oxidized nonetheless.

Likewise, the values of  $\kappa$  reported by Haensel for Cu agree with our measurements CuO rather than our measurements of Cu. The Haensel measurements were not made *in situ* and Haensel did not report taking any measures to prevent or minimize sample oxidation. The samples he used were as thin as 5 nm, so we presume that his samples were fully oxidized at the time of measurement.

## 5. Conclusion

We have used a laser-high-harmonics-based polarimeter to measure the optical constants of copper and copper (II) oxide in the range from 10 nm to 35 nm. Although the comparisons to some previous data sets for Cu show disagreement, we still have confidence that our data is correct. Firstly, the other data sets do not all agree with each other. Second, we are the only researchers to measure both copper metal and oxidized copper and show that those measurements are different. Third, our data for copper agree with the only other data set (that we are aware of) also measured *in situ* (albeit with limited wavelength coverage in the EUV), whereas our measurements for CuO match two data sets for which oxidation is likely to have occurred. These findings underscore the importance of controlling oxidation, which may have bearing also in the context of photolithography.

## Acknowledgement

This work was supported by the National Science Foundation (NSF) under grant number PHY-0457316.